AQRP Project 14-022

# Use of Satellite Data to Improve Specifications of Land Surface Parameters


By
Richard T. McNider, Kevin Doty and Yu Ling Wu, ESSC
University of Alabama – Huntsville
And
Pius Lee
NOAA Air Resources Laboratory
Min Huang
George Mason University


UAH

- **Specifying  surface characteristics which impact temperature. moisture and boundary layer dynamics are critical  to air quality modeling.**
- **Also critical to efficacy and efficiency of control strategy**

**Mixing Heights** – Underestimate of mixing heights can cause an over-estimate of the sensitivity of controls. Emission reductions confined to a smaller volume cause a larger reduction in ozone. A 30% error in mixing heights can produce 30% error in emission change impacts

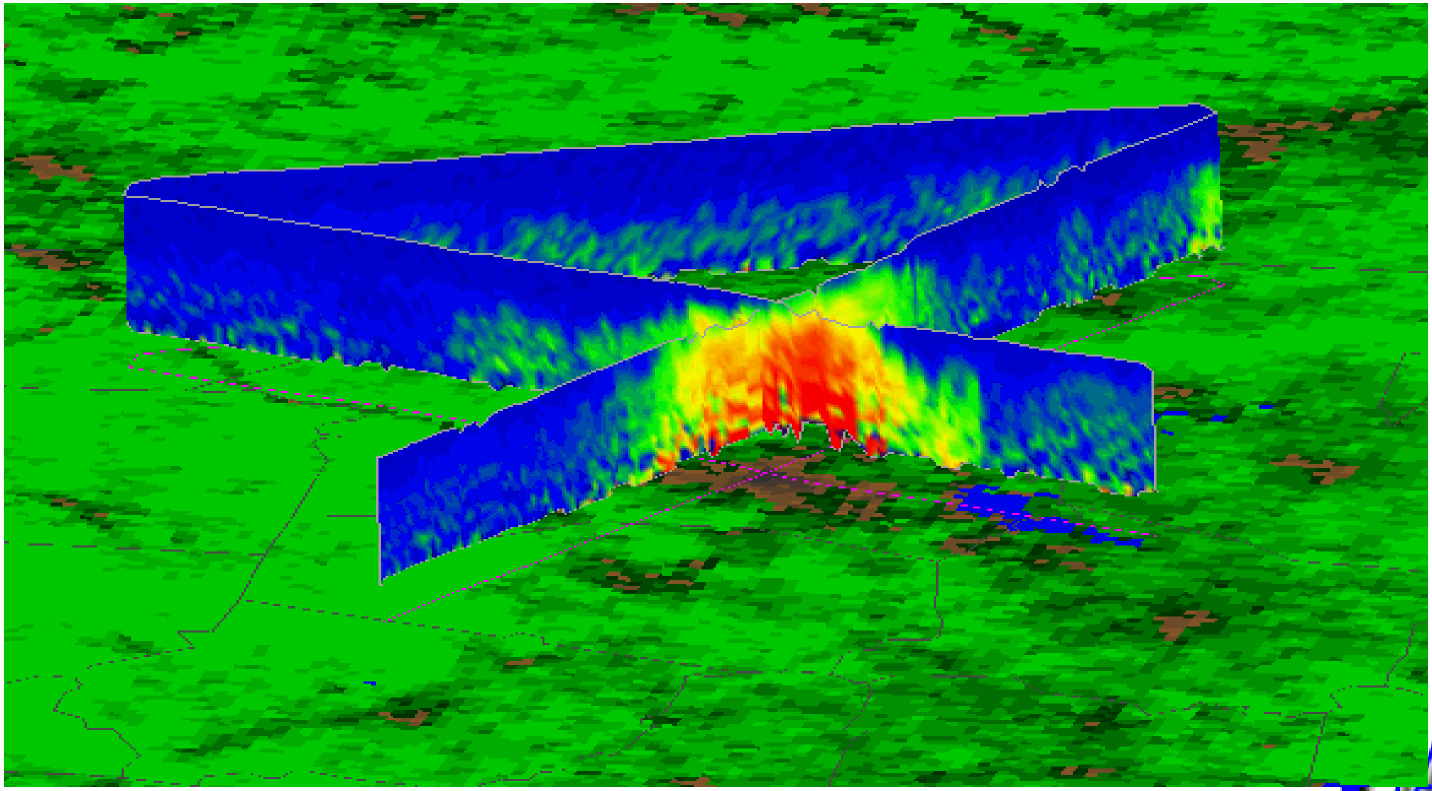

**Temperature –** over prediction of temperature can bias ozone controls toward NOx controls as thermal decomposition of increases slope of ozone/NOy curves.

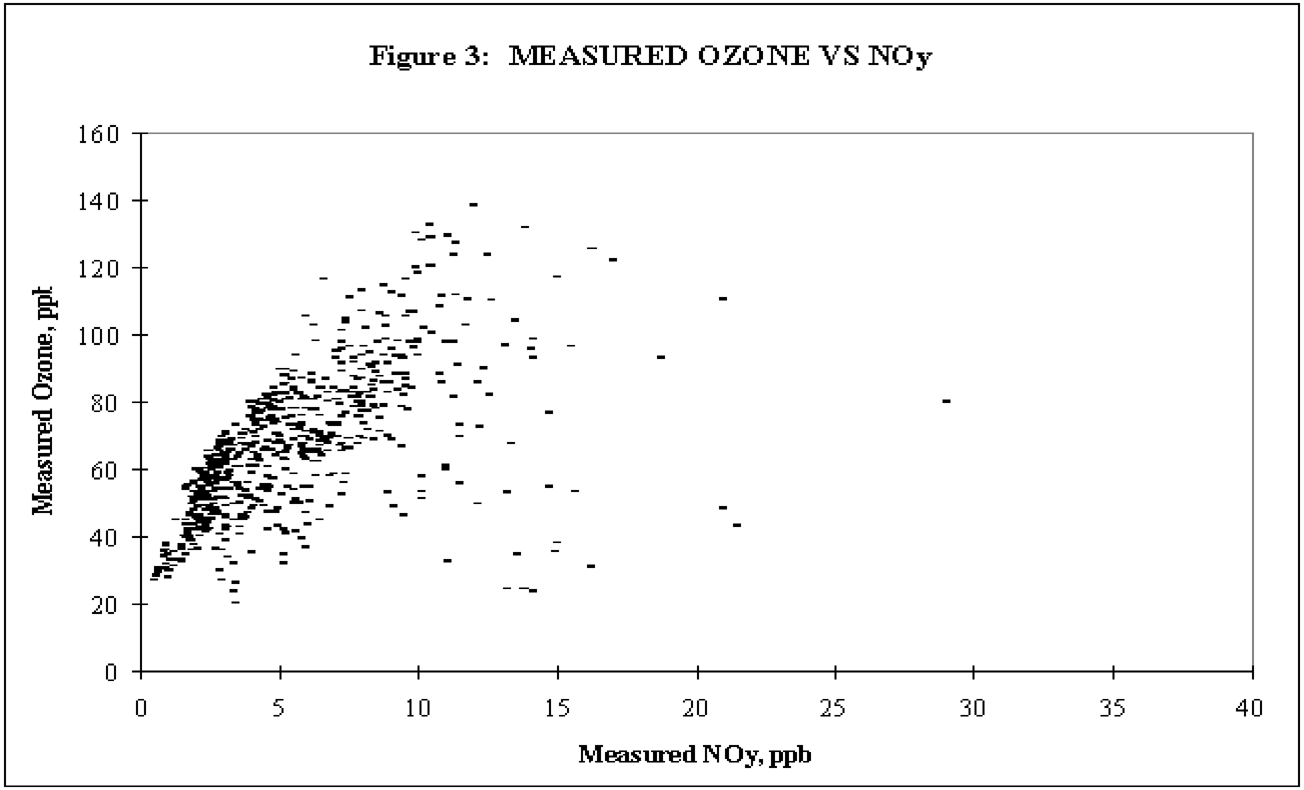

## Biogenic VOC and anthropogenic evaporative emissions are a strong function of temperature

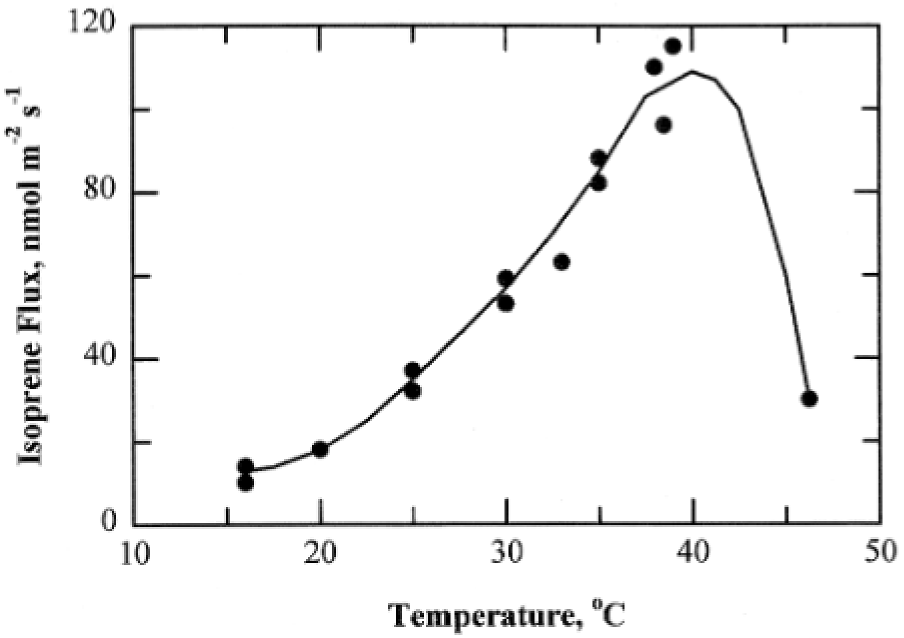


FIG. 4. Isoprene emissions in functions of leaf temperature for white oak (*Quercus alba*) leaves. Fluxes are expressed per unit leaf area.

from Fuentes et al BAMS 2000

# Moisture

Soil moisture impacts  NOx emissions.

Atmospheric moisture can impact dry chemistry and wet chemistry.

Pollutant uptake by plants is directly related to photosynthesis and transpiration. Under-estimation of moisture and associated surface loss can overestimate the role of long range transport in local air pollution levels.

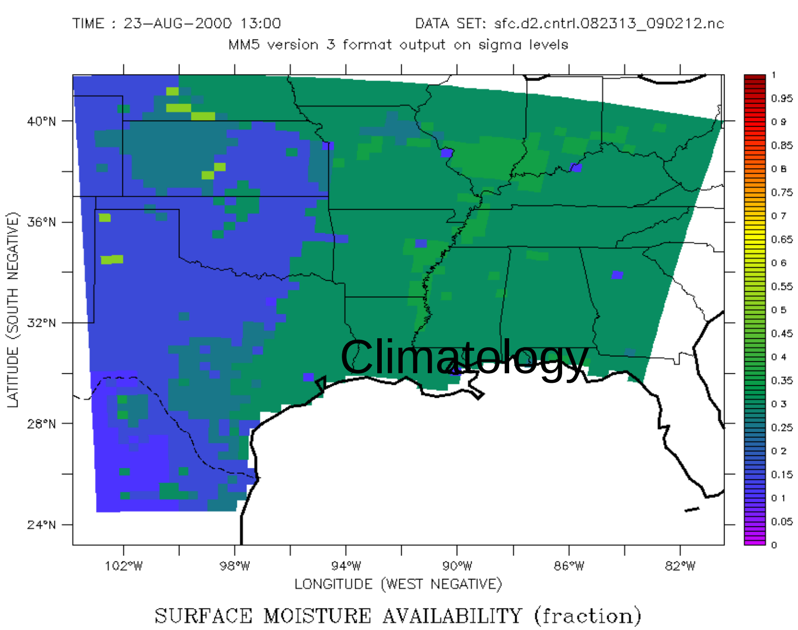


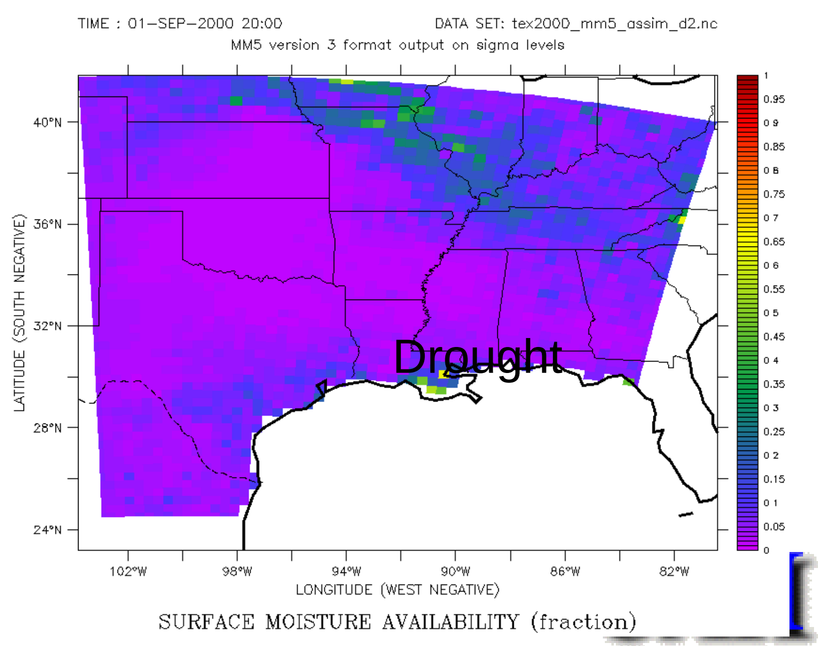

# Temperature and Moisture Modeling

Factors controlling surface temperatures and moisture are complex and many models have created complex land surface models that in the end require many ill defined parameters.

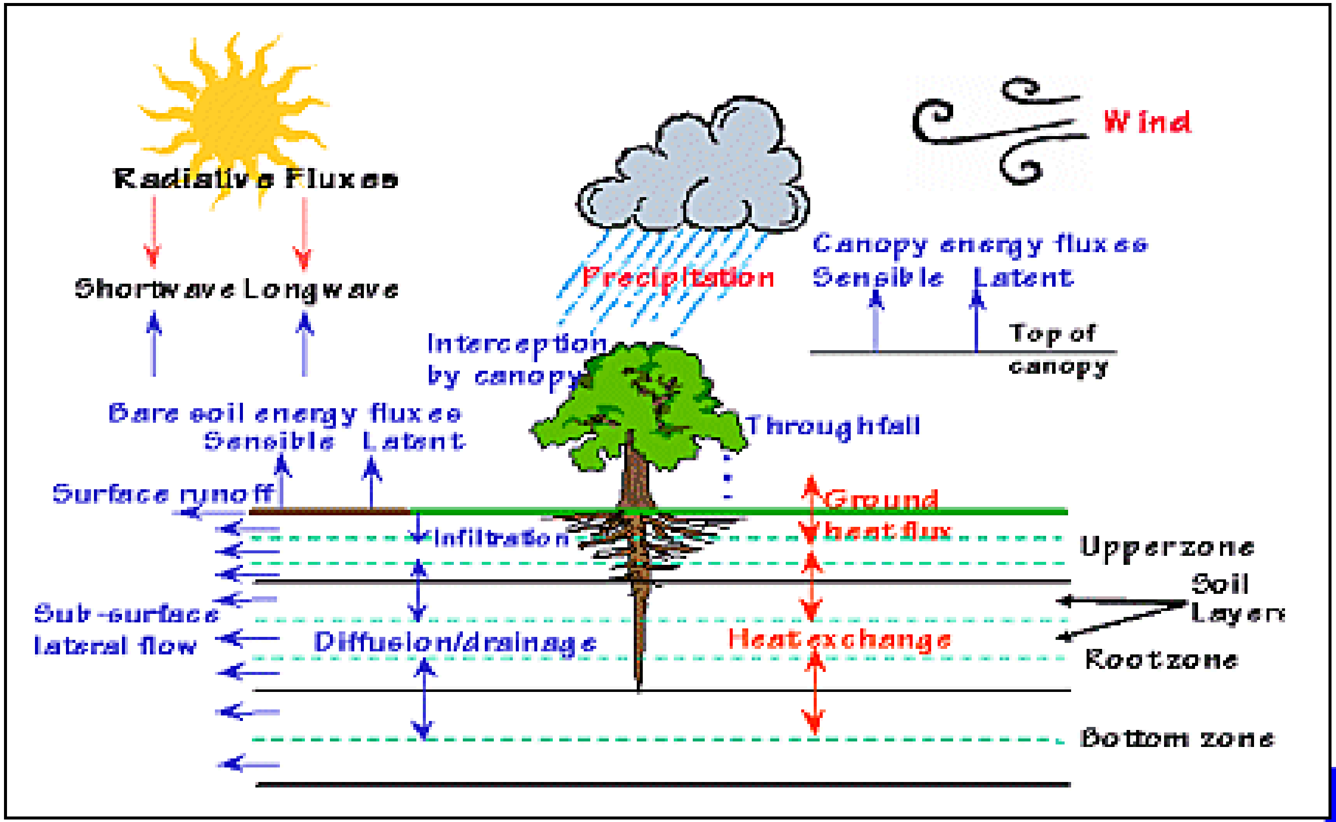


UAH

**Models have attempted to improve performance by developing improved land use classes (LUC) using in situ and satellite data**

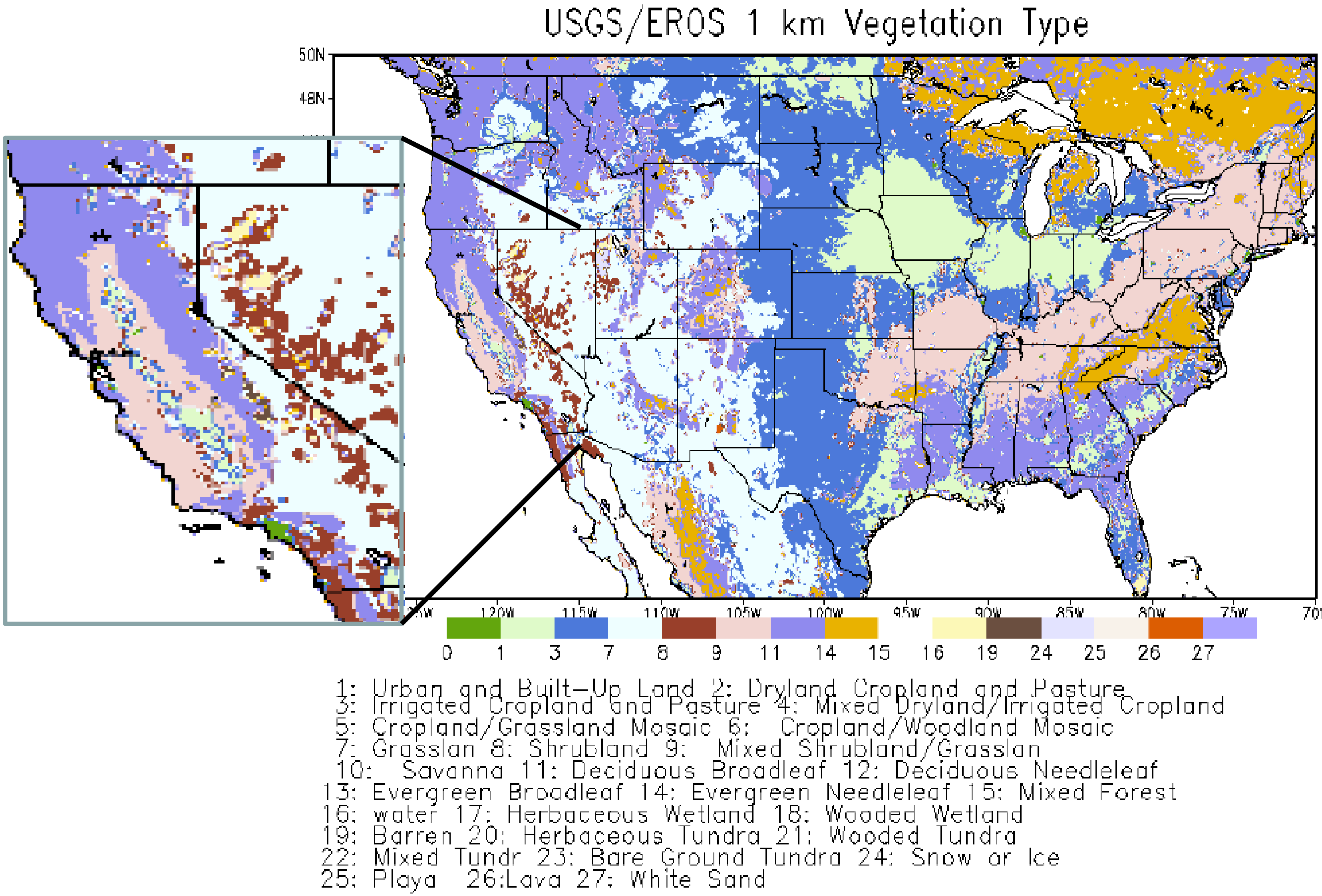

Unfortunately models don't use land surface classes directly. Physical parameters such as heat capacity, canopy resistance, surface moisture have to be defined for the Land Use Class

| | |
|---|---|
| Albedo - SFC albedo (in percentage) | RGL - Parameter used in radiation stress function |
| Z0 – Roughness Length (m) | HS - Parameter used in vapor pressure deficit |
| SHDFAC - Green vegetation fraction | SNUP - Threshold depth for 100% snow cover |
| NROOT - Number of root layers | LAI - Leaf area index (dimensionless) |
| RS - stomatal resistance (s m-1) | MAXALB - Upper bound on max albedo snow |

## Vegetation Parameters

| Category | Class | Albedo | Z0 | SHDFAC | NROOT | RS | RGL | HS | SNUP | LAI | MAXALB |
|---|---|---|---|---|---|---|---|---|---|---|---|
| Urban and Built-Up Land | 1 | 0.15 | 1.00 | 0.10 | 1 | 200. | 999. | 999.0 | 0.04 | 4 | 40 |
| Dryland Cropland and Pasture | 2 | 0.19 | 0.07 | 0.80 | 3 | 40. | 100. | 36.25 | 0.04 | 4 | 64 |
| Irrigated Cropland and Pasture | 3 | 0.15 | 0.07 | 0.80 | 3 | 40. | 100. | 36.25 | 0.04 | 4 | 64 |
| Mixed Dryland/Irrigated Cropland and Pasture | 4 | 0.17 | 0.07 | 0.80 | 3 | 40. | 100. | 36.25 | 0.04 | 4 | 64 |
| Cropland/Grassland Mosaic | 5 | 0.19 | 0.07 | 0.80 | 3 | 40. | 100. | 36.25 | 0.04 | 4 | 64 |
| Cropland/Woodland Mosaic | 6 | 0.19 | 0.15 | 0.80 | 3 | 70. | 65. | 44.14 | 0.04 | 4 | 60 |
| Grassland | 7 | 0.19 | 0.08 | 0.80 | 3 | 40. | 100. | 36.35 | 0.04 | 4 | 64 |
| Shrubland | 8 | 0.25 | 0.03 | 0.70 | 3 | 300. | 100. | 42.00 | 0.03 | 4 | 69 |
| Mixed Shrubland/Grassland | 9 | 0.23 | 0.05 | 0.70 | 3 | 170. | 100. | 39.18 | 0.035 | 4 | 67 |
| Savanna | 10 | 0.20 | 0.86 | 0.50 | 3 | 70. | 65. | 54.53 | 0.04 | 4 | 45 |
| Deciduous Broadleaf Forest | 11 | 0.12 | 0.80 | 0.80 | 4 | 100. | 30. | 54.53 | 0.08 | 4 | 58 |
| Deciduous Needleleaf Forest | 12 | 0.11 | 0.85 | 0.70 | 4 | 150. | 30. | 47.35 | 0.08 | 4 | 54 |
| Evergreen Broadleaf Forest | 13 | 0.11 | 2.65 | 0.95 | 4 | 150. | 30. | 41.69 | 0.08 | 4 | 32 |
| Evergreen Needleleaf Forest | 14 | 0.10 | 1.09 | 0.70 | 4 | 125. | 30. | 47.35 | 0.08 | 4 | 52 |
| Mixed Forest | 15 | 0.12 | 0.80 | 0.80 | 4 | 125. | 30. | 51.93 | 0.08 | 4 | 53 |
| Water Bodies | 16 | 0.19 | 0.001 | 0.00 | 0 | 100. | 30. | 51.75 | 0.01 | 4 | 70 |
| Herbaceous Wetland | 17 | 0.12 | 0.04 | 0.60 | 2 | 40. | 100 | 60.00 | 0.01 | 4 | 35 |
| Wooded Wetland | 18 | 0.12 | 0.05 | 0.60 | 2 | 100. | 30. | 51.93 | 0.02 | 4 | 30 |
| Barren and Sparsely Vegetated | 19 | 0.12 | 0.01 | 0.01 | 1 | 999. | 999. | 999.0 | 0.02 | 4 | 69 |
| Herbaceous Tundra | 20 | 0.16 | 0.04 | 0.60 | 3 | 150. | 100. | 42.00 | 0.025 | 4 | 58 |
| Wooded Tundra | 21 | 0.16 | 0.06 | 0.60 | 3 | 150. | 100. | 42.00 | 0.025 | 4 | 55 |
| Mixed Tundra | 22 | 0.16 | 0.05 | 0.60 | 3 | 150. | 100. | 42.00 | 0.025 | 4 | 55 |
| Bare Ground Tundra | 23 | 0.17 | 0.03 | 0.30 | 2 | 200. | 100. | 42.00 | 0.02 | 4 | 65 |
| Snow or Ice | 24 | 0.70 | 0.001 | 0.00 | 1 | 999. | 999. | 999.0 | 0.02 | 4 | 75 |

**Can we perhaps use satellite observed skin temperatures to specify parameters in land use classes so that the model in turn reproduces the observed skin temperatures**

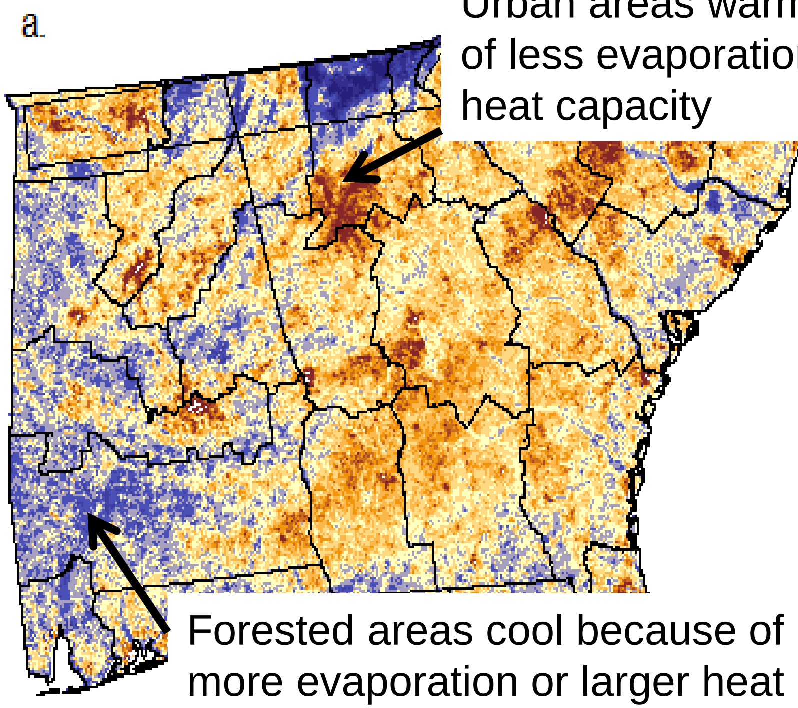


Urban areas warmer because of less evaporation or smaller heat capacity

Forested areas cool because of more evaporation or larger heat capacity

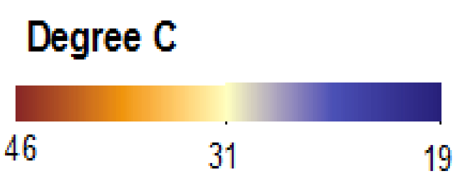


**MODIS Skin Temperatures**

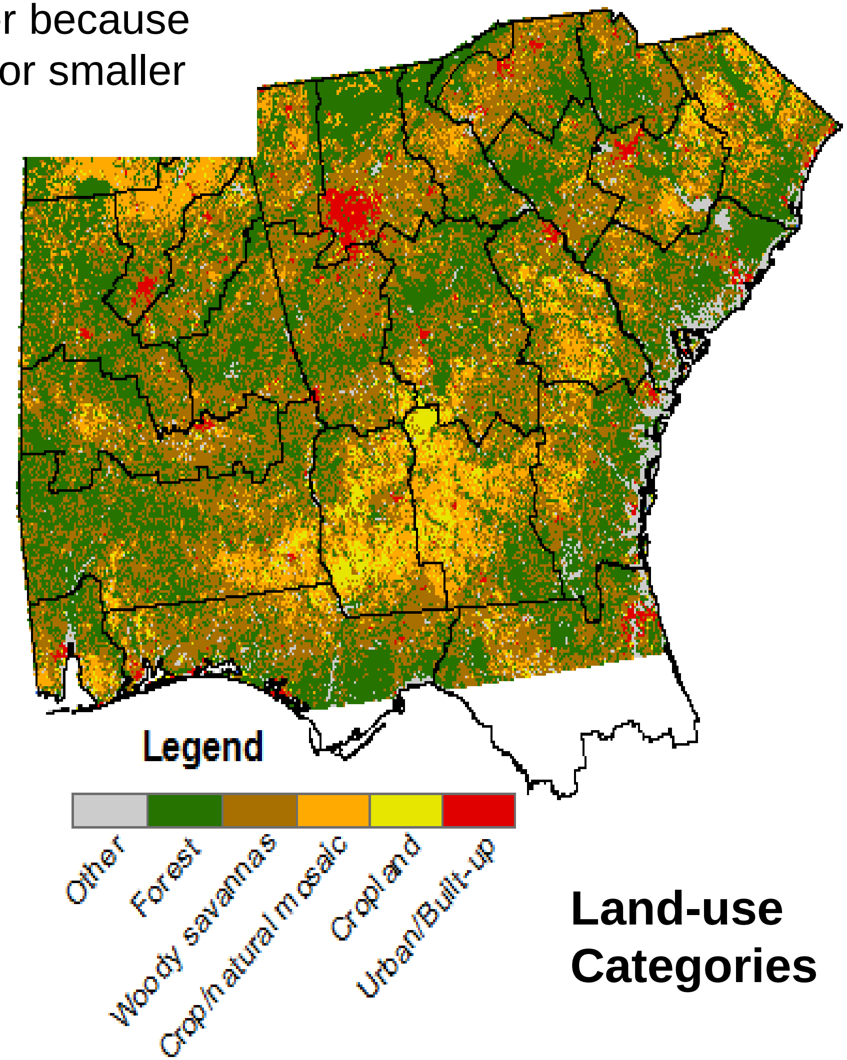


**Land-use Categories**

From Ellenburg 2015

Climate models must use complex models for energy and water balance models to run unattended for years.

In weather forecasting and air pollution applications the better approach may be to use simple models highly constrained by observations.

This may be especially true for retrospective studies such as SIP periods.

Examples

McNider et al 1994 MWR Moisture adjustment using satellite time tendency data

Anderson et al 1997(ALEXI) JAM moisture adjustment using satellite data

Pleim and Xiu 2003 JAM Moisture adjustment using surface obs

McNider et al 2005 JCAM Heat capacity/thermal inertia adjustment.

UAH

We have taken a different approach and have embraced simple models but highly constrained by observations. Simple model is based on the Pleim-Xiu scheme in WRF.

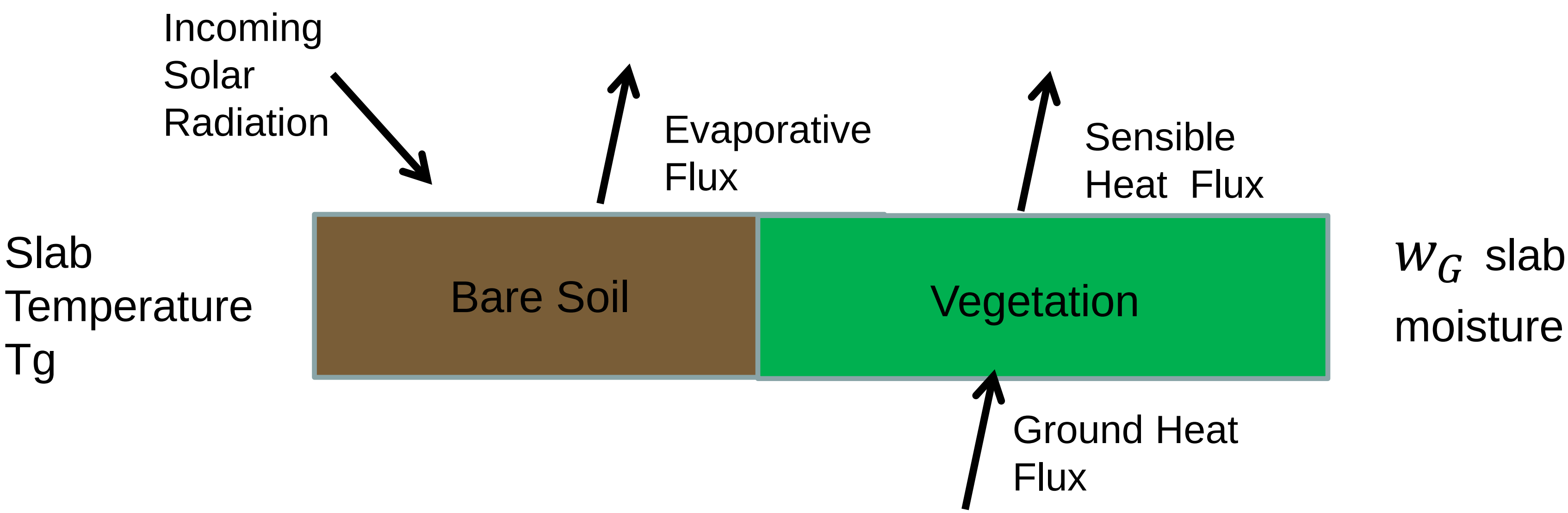


Original Pleim-Xiu used differences between National Weather Service observations and model temperatures to nudge moisture in the proper direction.

$$\Delta w_G = \alpha_1 \left( T^A - T^F \right) + \alpha_2 \left( RH^A - RH^F \right)$$

Here we will constrain the Pleim-Xiu scheme with satellite data

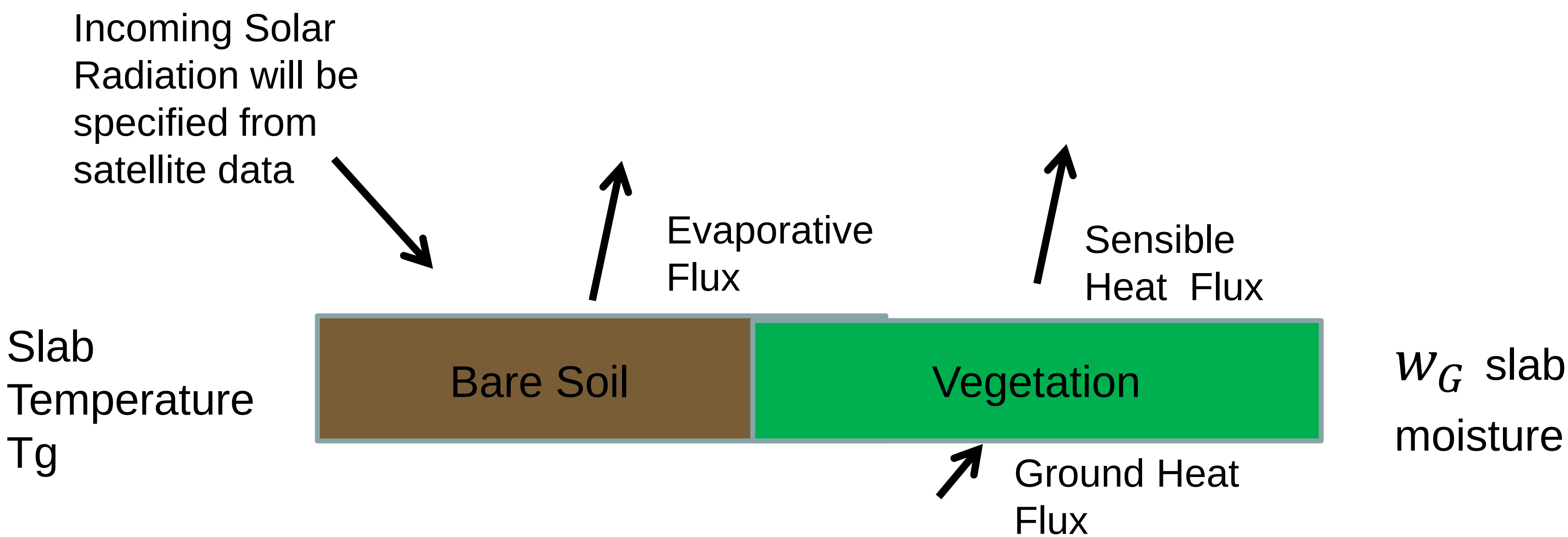


We will use differences between satellite skin temperature observations and model skin temperatures to nudge moisture in the proper direction.

$$\Delta w_G = \beta_1 (T_S^{Sat} - T_S^{Mod})_{Morning}$$

We will try to use differences in the satellite and model skin to nudge the slab heat capacity $C_g$ (thermal resistance) (McNider et al . 2005)

$$\Delta C_g = \beta_2 \ (T_S^{Sat} - T_S^{Mod})_{Evening}$$

The satellite observes a skin or radiating temperature while the original Pleim-Xiu scheme only provided a slab temperature associated with a finite heat capacity - $c_g$

$$c_g \frac{\partial T_G}{\partial t} = R_L + (1-\alpha_s) R_s - \varepsilon \sigma T_S^4 - H - E - G$$

Following Makaro 2011 we take the limit of $c_g$ approaching 0 to obtain a infinitely thin surface.

$$R_L + (1-\alpha_s) R_s - \varepsilon \sigma T_S^4 - H - E - S = 0$$

We use root finding techniques to recover a true skin temperature, $T_s$ .

UAH

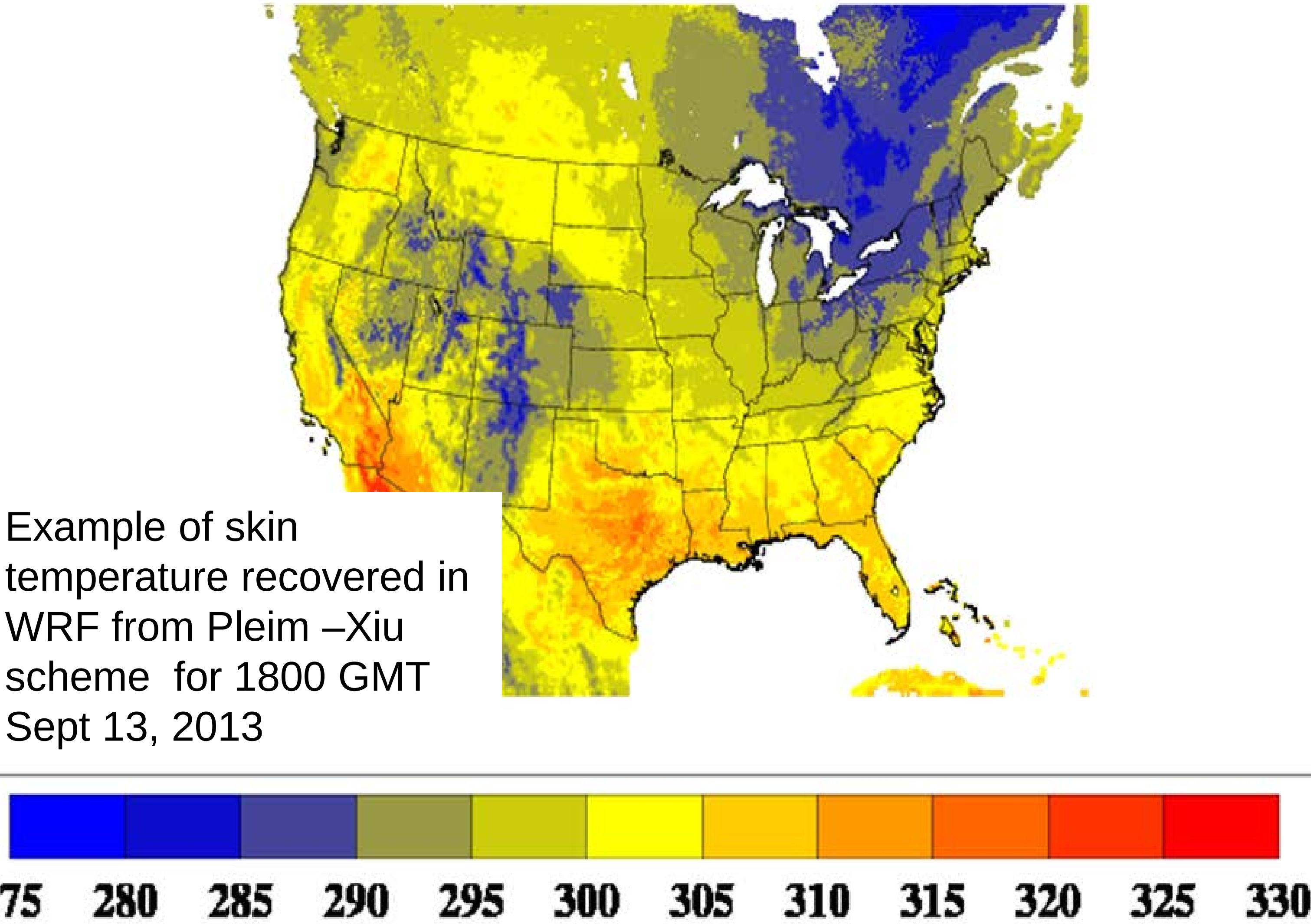


Example of skin temperature recovered in WRF from Pleim –Xiu scheme for 1800 GMT Sept 13, 2013

The first step in using the skin temperatures from the satellite to improve moisture or heat capacity is to ensure that the surface energy budget in the model and the surface the satellite sees are being forced by the same solar forcing , $R_{s.}$

$$c_g \frac{\partial T_G}{\partial t} = R_L + (1 - \alpha_s) R_s - \varepsilon \sigma T_s^4 - H - E - G$$

Solar insolation during the day usually the biggest term in the equation.

We use a satellite derived insolation product originally developed by Gautier and Diak 1980.

UAH

# September 2013 Discovery AQ

[redacted]

WRF

New NOAA Product

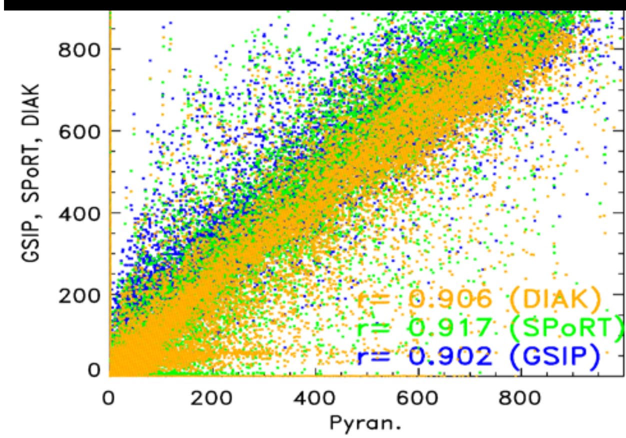


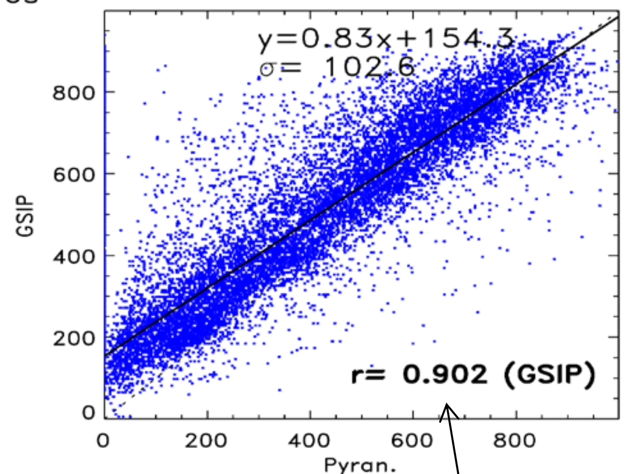


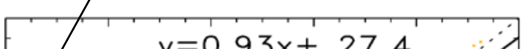


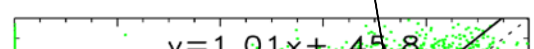

New Water Vapor Dependent Product

Original UAH Product

UAH

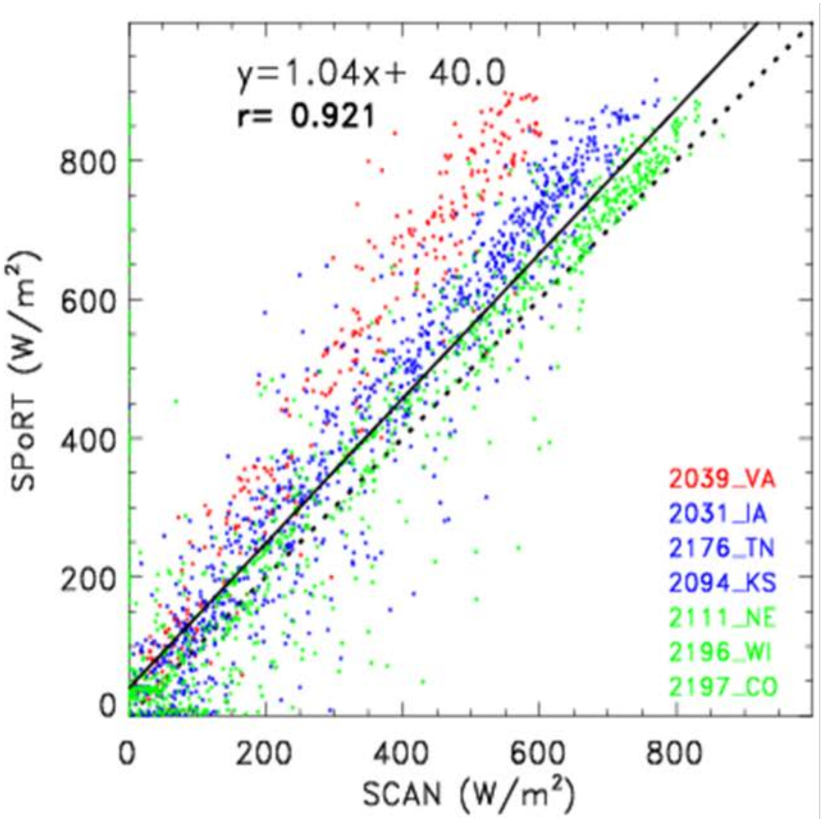


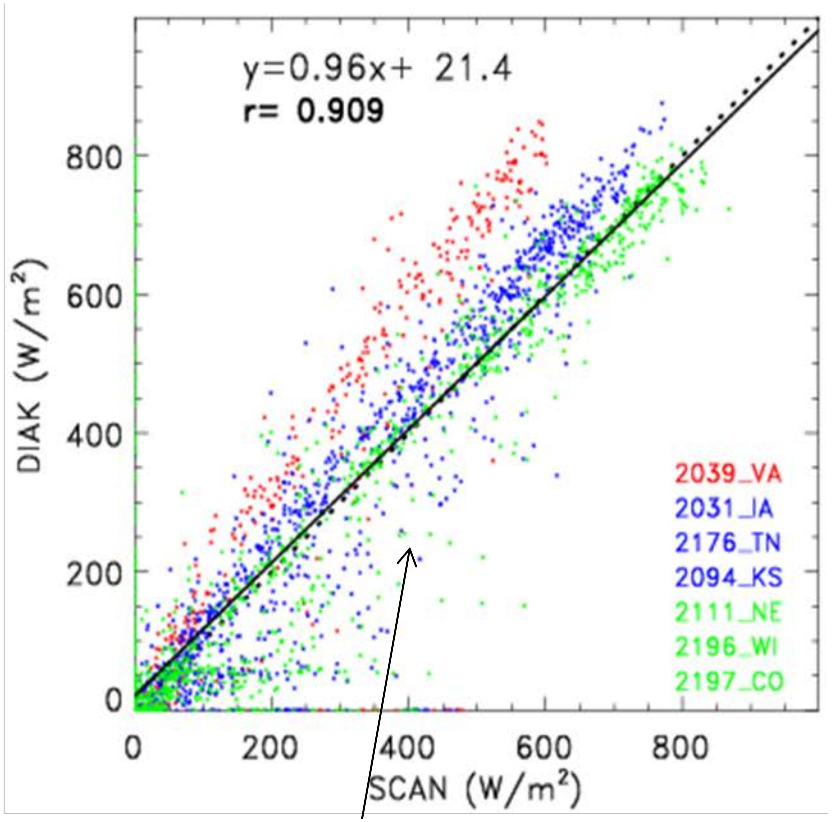


Original UAH Product

With variable precipitable water

If we don’t find the fundamental source of the over-prediction in the East we will use a calibration developed by Pour –Biazar under another AQRP project

UAH

The next step in the use of satellite skin is to develop satellite skin temperature products that can be used in the moisture and heat capacity nudging discibed above.

In the past our group had used a UAH/NASA skin temperature product. However, it was based on a sounder instrument and only had a resolution of 10 km or so. It also had some striping issues.

Thus, for this Texas AQRP project we had proposed to use a new NOAA GSIP skin temperature product.

While it looked good in the East we found unrealistic temperatures in the west.

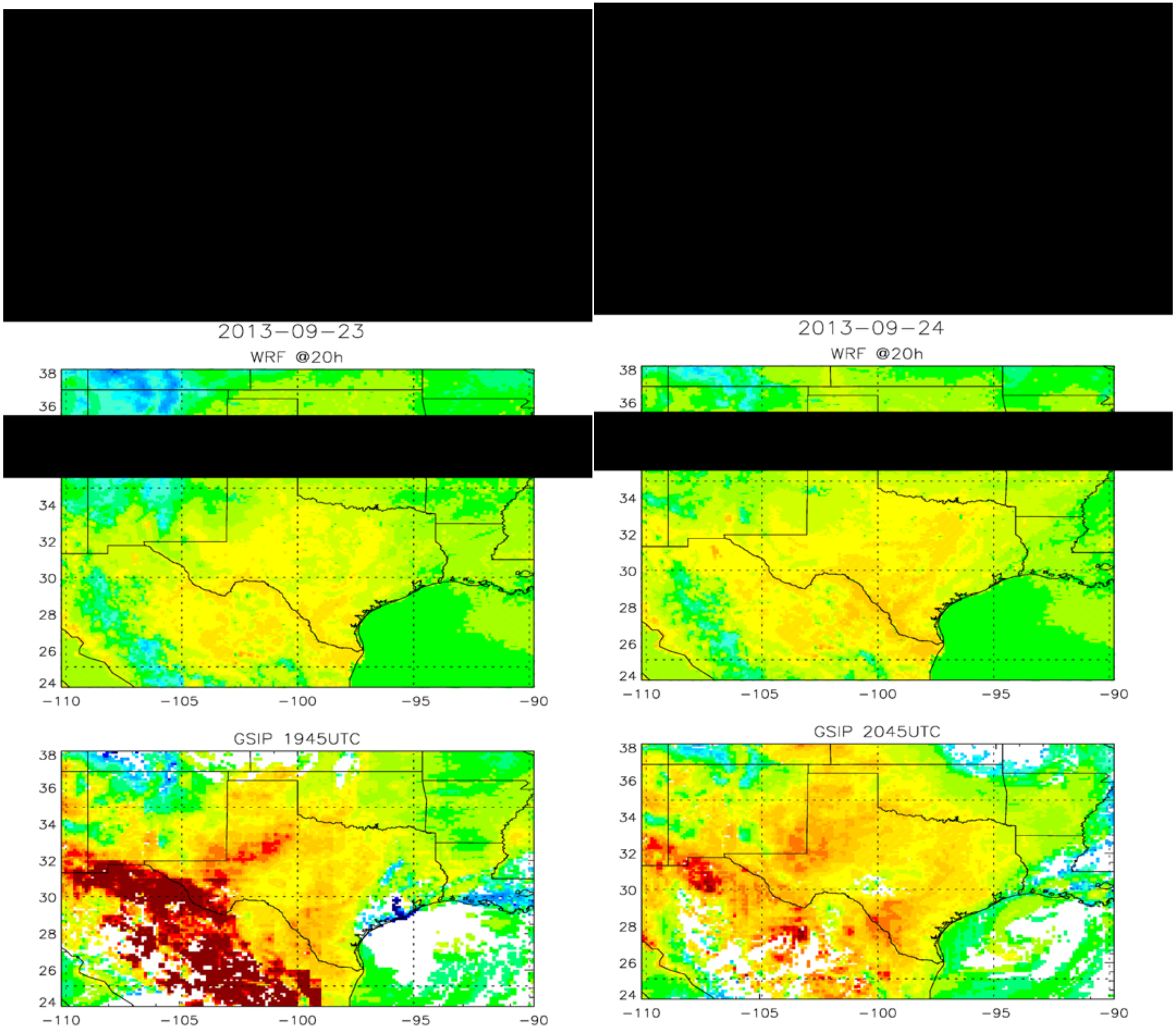


Fig. 6. Skin Temperature, from top to bottom—WRF, GSIP, and MODIS(Aqua). Left panels are for Sep 23, 2013 (Aqua overpass time was 19:45&19:50 GMT),

UAH

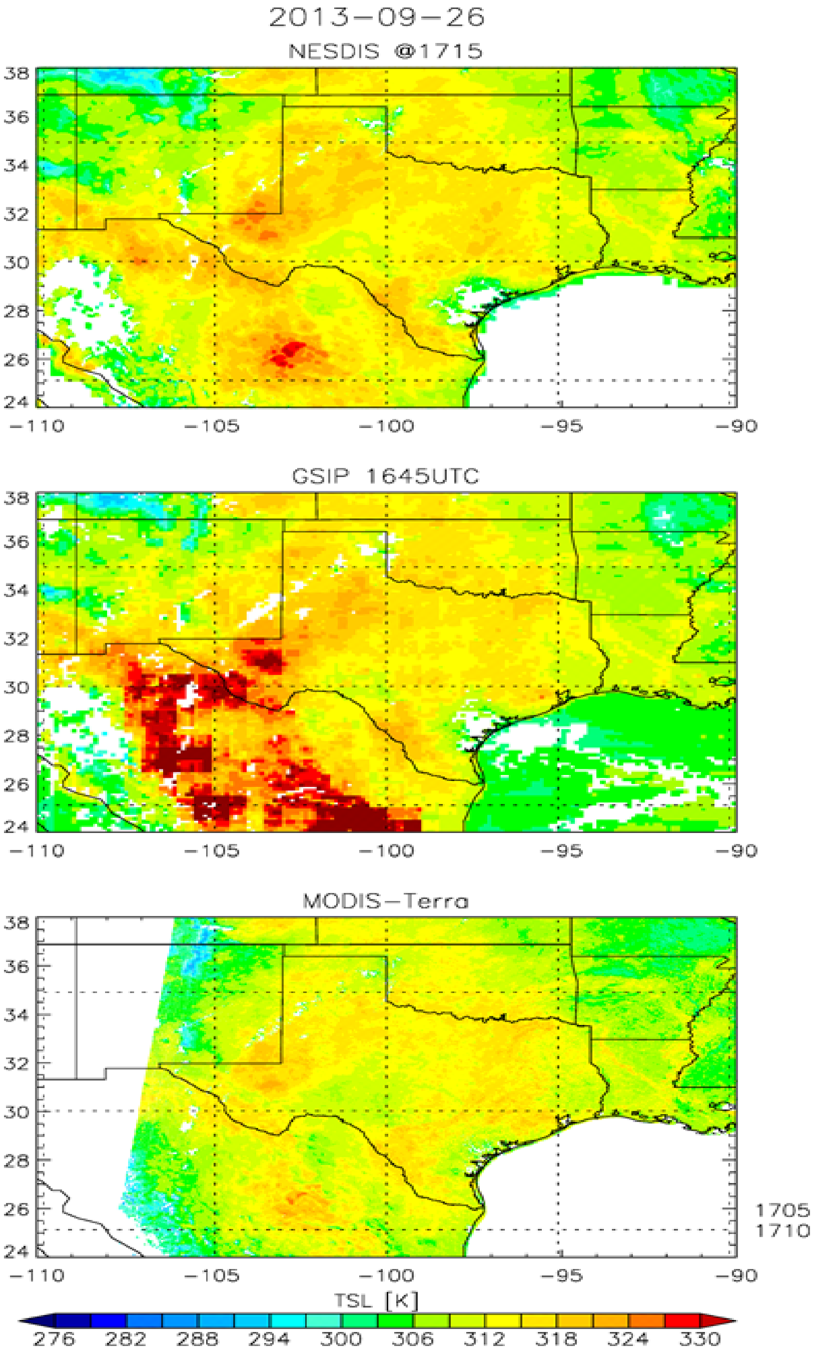


New NOAA Skin Temperature Product
Courtesy Chris Hain

GSIP NOAA Skin Temperature Product

MODIS Skin Temperature Product

UAH

The images above of skin temperatures show that while the patterns may be similar there are absolute differences in values. This is in part due to lack of IR sensor calibration on aircraft and satellites. Also, due to offsets in model skin temperatures to reality.

There are many papers which have attempted to directly assimilate observed skin temperatures with little success. Our group and the ALEXI group have always relied on the use of skin tendencies which avoid issues of offsets/calibration.

Under this activity we will develop a quasi-observed field tied to the model skin temperature but using observed skin temperature tendencies.

$$Tqo\,(x,y,t+\Delta t) = Tqm(x,y,t) + \Delta t\left(\frac{\partial To(x,y,t)}{\partial t}\right)$$

quasi-observed skin temperature

model skin temperature

observed skin temperature tendencies

UAH

Potential of Skin Temperature to Improve WRF Performance

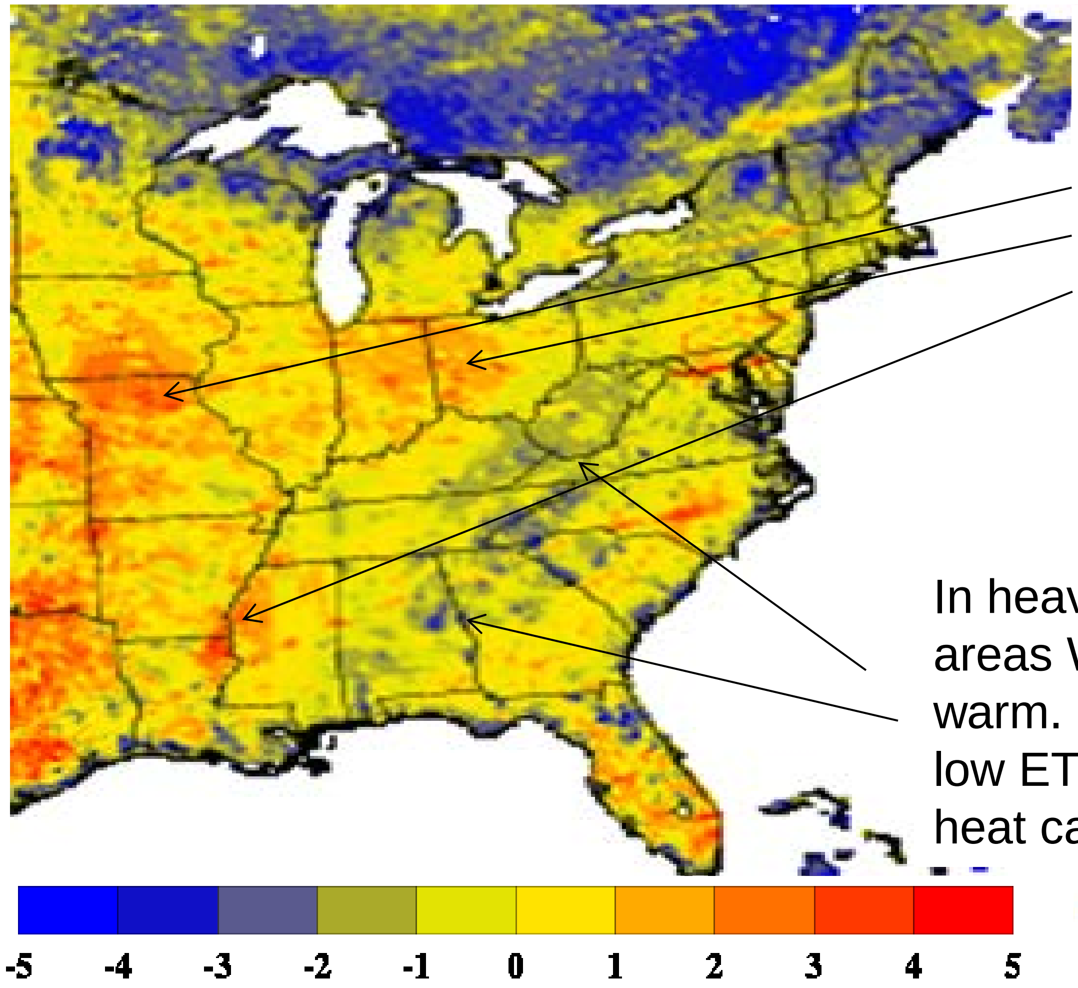


In September corn has been harvested and no longer transpiring. WRF is cooler than satellite likely has too much ET or too large heat capacity

In heavily forested areas WRF is too warm. May have too low ET or too small heat capacity

Difference between GOES Skin Temperature and WRF Control

Model Test (Sept 1-Sept 30) period Includes DISCOVERY AQ
NOAA ARL is using aircraft data for model evaluation

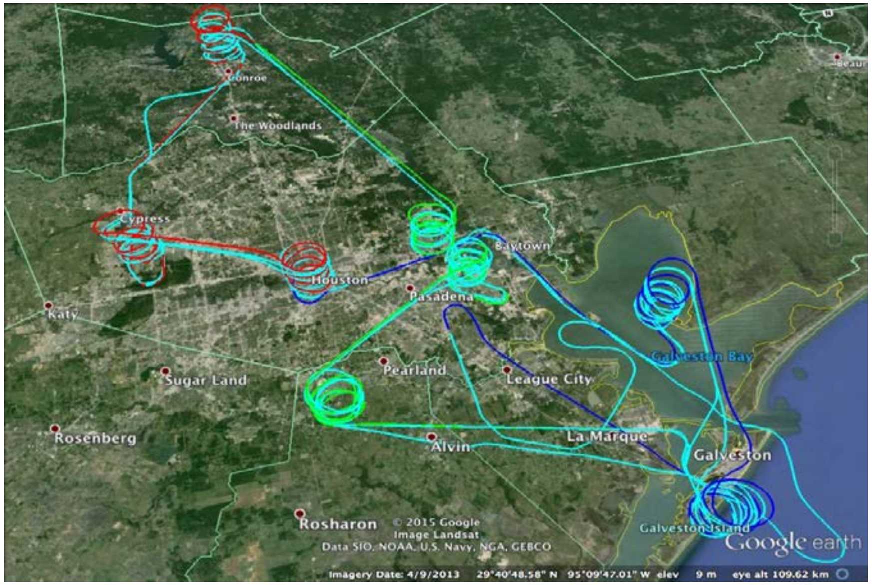


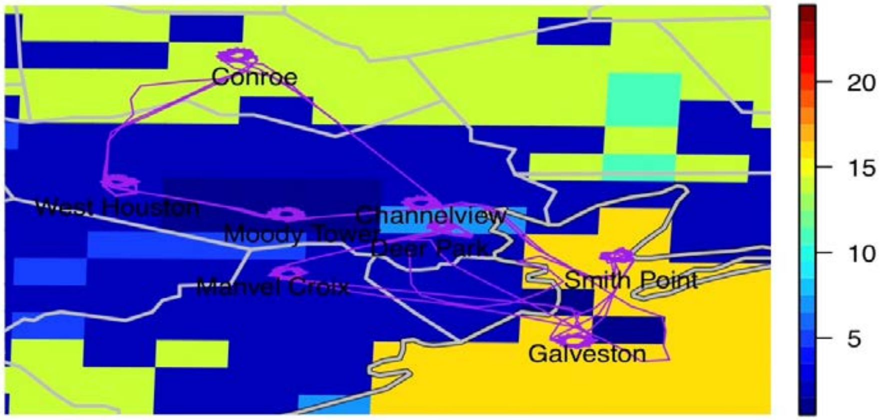


Fig. 12. NASA P3-B flight path on September 25, 2013. The flight path is overlaid on Google Earth images (upper) and 24-category USGS land use data on WRF grid (lower). USGS land use types are specified in Table 2.

NASA P3 has downward looking IR radiometer

NOAA ARL is making comparisons of modeled and satellite skin temperature with aircraft skin temperature

NASA Aircraft Skin Temperature

WRF Skin Temperature

Satellite Skin Temperature

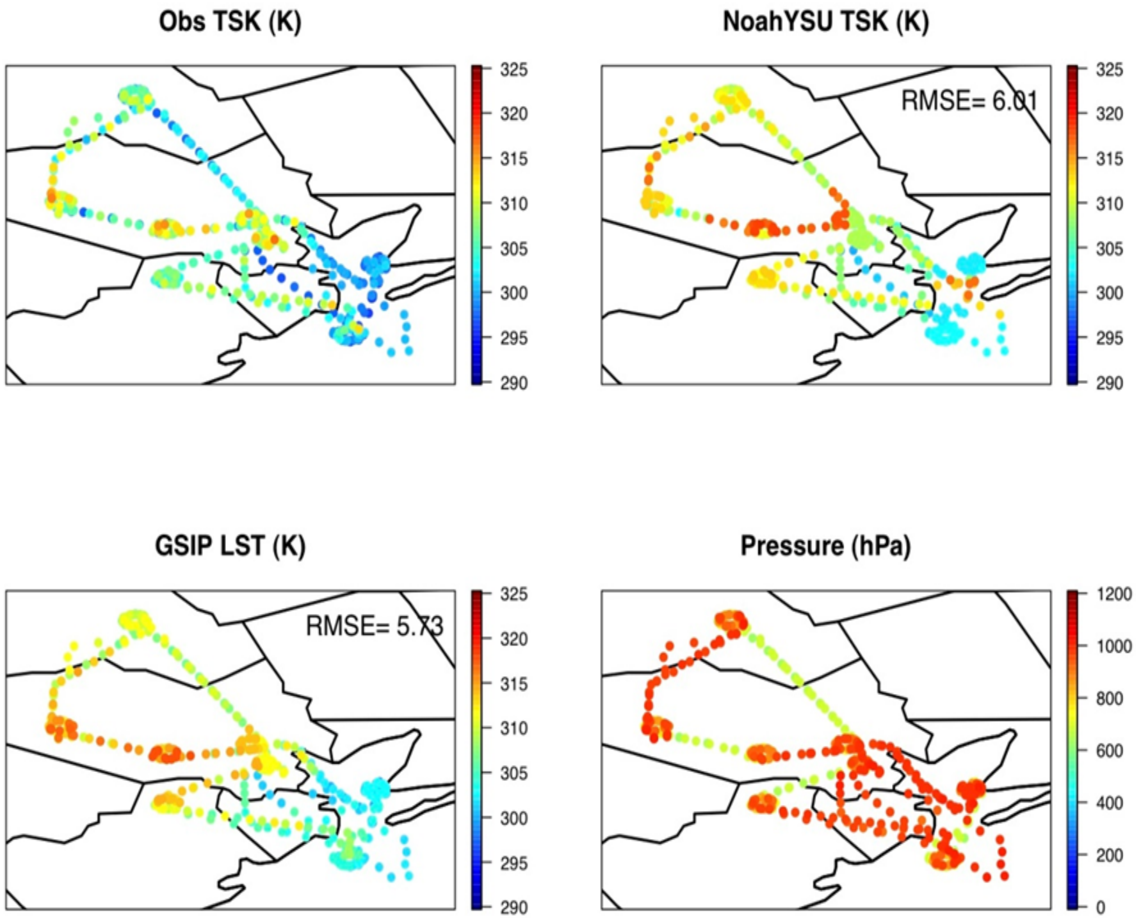


UAH

Schedule:

1. Plan First Test of Moisture Skin Temperature Assimilation Technique by July 15

2. Heat Capacity Assimilation in August

UAH

Thanks to Cyril Durrenberger, Bright Dornblaser, and Vince Torres for comments and improved focus of the project

UAH